Palaeoentomology 009 (3): 228–242
https://www.mapress.com/pe/

Article

ISSN 2624-2826 (print edition)
PALAEOENTOMOLOGY
ISSN 2624-2834 (online edition)

https://doi.org/10.11646/palaeoentomology.9.3.6
http://zoobank.org/urn:lsid:zoobank.org:pub:08FF98F1-FF60-43DE-9A8A-A12F82B9F509

The centipede *Cryptops* from Baltic amber (Chilopoda: Scolopendromorpha): phylogenetic analysis using combined morphological and molecular data

CAMILLE VIDAL-MARTY[1], GREGORY D. EDGECOMBE[2,*] & GONZALO GIRIBET[3]
[1]*Université Claude Bernard Lyon 1, ENSL, UMR CNRS 5276 LGLTPE, F-69622, Villeurbanne, France*
[2]*The Natural History Museum, Cromwell Road, London SW7 5BD, United Kingdom*
[3]*Museum of Comparative Zoology, Department of Organismic & Evolutionary Biology, Harvard University, 26 Oxford Street, Cambridge, Massachusetts 02138, USA*
camille.vidal--marty@etu.univ-lyon1.fr
g.edgecombe@nhm.ac.uk; https://orcid.org/0000-0002-9591-8011
ggiribet@g.harvard.edu; https://orcid.org/0000-0002-5467-8429
**Corresponding author*

Abstract

Two specimens of scolopendromorph centipedes from Eocene Baltic amber provide a confidently documented fossil record of the blind family Cryptopidae. The fossil material, illustrated via light microscopy and microcomputed tomography, is assigned to the extant genus *Cryptops* Leach, 1814, based on diagnostic morphological characters such as the absence of eyes, 21 leg-bearing segments with strongly delimited pre- and metatergites, oblique sutures and lateral crescentic sulci on the tergites, and robust, spiniform setae on the ultimate legs. A distinctive pattern of sutures on the first trunk tergite supports conspecificity of the fossil material and a unique combination of characters allows distinction from extant species. Phylogenetic analysis of a dataset for blind Scolopendromorpha incorporates 61 morphological characters for 41 species (37 extant, four extinct) with sequence data for two nuclear ribosomal and two mitochondrial loci for the extant species. The total-evidence maximum likelihood tree places the fossils within total-group *Cryptops* in a framework of strongly supported extant clades. The fossils constrain a minimum divergence date for the genus to the late Eocene (Priabonian) according to the age of Baltic amber, although geographic structure within extant clades of *Cryptops* and previous molecular estimates suggest this is a conservative minimum. The discovery supplements the sparse Cenozoic fossil record for Scolopendromorpha and illustrates an application of amber inclusions as temporal calibration points in centipede phylogeny.

Keywords: Scolopendromorpha, Cryptopidae, Baltic amber, Eocene

Introduction

The centipede order Scolopendromorpha comprises over 700 extant species classified in five families: Cryptopidae, Mimopidae, Plutoniumidae, Scolopocryptopidae and Scolopendridae. Cryptopidae is one of the three blind families that constitute the clade Tykhepoda (Benavides *et al*., 2023), and consists of a single genus, *Cryptops* Leach, 1814. More than 170 species of *Cryptops* are classified in four subgenera: the nominate subgenus *Cryptops*, *Paracryptops* Pocock, 1891, *Trigonocryptops* Verhoeff, 1906, and *Haplocryptops* Verhoeff, 1934 (Schileyko *et al*., 2020). The monophyly of Cryptopidae is strongly supported by Sanger-based sequencing of four markers, including nuclear ribosomal and mitochondrial ribosomal and protein-coding genes (Vahtera *et al*., 2012, 2013; Edgecombe *et al*., 2020) as well as phylotranscriptomic data (Benavides *et al*., 2023). It is also supported by morphological datasets (Vahtera *et al*., 2013), and the family/genus are readily diagnosed by characters such as 21 leg-bearing segments, trunk tergites with lateral crescentic sulci, strong division of pre- and metatergites, a sieve-type gizzard, strong setae on the ultimate legs, and saw teeth on the ultimate leg tibia and tarsus 1. Variability in taxonomic characters in *Cryptops*, one of the most species-rich centipede genera, has been reviewed by Lewis (2009).

Scolopendromorpha dates to at least the Late Carboniferous, being represented by *Mazoscolopendra richardsoni* Mundel, 1979, in the Mazon Creek deposits in Illinois, USA (Haug *et al*., 2014). Baltic amber centipedes have barely been studied since the 1850s, the only reported *Cryptops* in this Eocene amber being an unnamed, unillustrated species (Bachofen-Echt, 1942). Cryptopidae is also known from specimens reported from late Oligocene-early Miocene Mexican amber (Cadenas-Amaya *et al*., 2025). Only recently have fossils of Chilopoda in amber started to be studied again

 Submitted: 12 Jan. 2026; accepted by D.-Y. Huang: 3 Jun. 2026; published: 29 Jun. 2026

as calibrations for scolopendromorph phylogeny using combined morphological and molecular data (Edgecombe *et al*., 2023).

This study aims to document the morphology of two amber-preserved *Cryptops* specimens. We describe and compare these Baltic amber specimens to extant taxa and code morphological characters in a phylogenetic analysis of the blind Scolopendromorpha clade, combining those data with already available multilocus molecular sequence data for all sampled extant species.

Material and methods

Fossil material

This study examines two cryptopid specimens preserved in amber, one from the Museum of Nature Hamburg, the other from the fossil arthropod collection of the Natural History Museum, London. They are catalogued under collection numbers GPI C. Gröhn 623 and NHMUK 014872695, respectively. The latter is a historic specimen transferred from the Museum Stantien & Becker (*ex*. No. 13497).

The studied specimens come from East Prussia and the Samland region (south of the Baltic Sea). Most amber with inclusions comes from the Blue Earth Layer, an Eocene glauconitic marine sediment (Priabonian, upper Eocene; see discussion on the age of the amber in Ross *et al*., 2026). The amber formed in oak-pine forests that thrived during the Eocene Climatic Optimum (Wolfe *et al*., 2009). The exact origin of the amber cannot be pinpointed, as it is recovered from both coastal and offshore areas, typically deposited in fine-grained marine sediments (Poinar, 1992).

Light microscopy

Focus-stacked images were acquired using a Hirox HRX-01 digital microscope with a motorized HR-2500E high-range lens system featuring a triple-objective configuration (20× to 2500× magnification). Imaging was performed in "Polarised light" mode using a Hirox High Intensity LED light source. Image stacks were processed with Helicon Focus Pro (version 8.3.4) and edited in Krita 5.2.9.

Micro-computed tomography

Micro-computed tomography (micro-CT) was performed on one amber inclusion (GPI C. Gröhn 623) with a Zeiss Xradia Versa 520 CT system in the Imaging and Analysis Centre at The Natural History Museum, London (UK). X-rays were produced from a tungsten source operating at 120 kV and 83.3 μA. Two scans were performed: an overall body view and a close-up of the head and anterior part of the trunk. Each scan acquired between 1,900 and 3,200 projections over a full 360° rotation. Imaging was conducted using a 0.4× objective lens, with exposure times ranging from 3 to 7 seconds per projection. The reconstructed volumetric data were processed in *Thermo Fisher Avizo* version 2022.2 (Visualization Sciences Group, Bordeaux, France). Two-dimensional slice stacks were generated, segmented, and reoriented to produce three-dimensional visualizations of the specimen along the X, Y, and Z axes. The dataset associated with the illustrated 3D reconstruction is available through Zenodo at the following link: https://zenodo.org/records/20081624. 3D reconstructions are also available through MorphoMuseum at the following link: https://morphomuseum.com/specimenfiles/view/1927/2e6a1d6a

Morphological data

The morphological dataset analyzed in this study builds on the 53-character matrix of Edgecombe *et al*. (2023) (Appendices 1, 2). Sixty-one characters were coded for 41 species, including three outgroups (15 taxa newly added, mostly species of *Cryptops*), in Mesquite 3.81 (Maddison & Maddison, 2025); the 37 extant species were selected in part based on the availability of molecular sequence data (Table 1). The morphological dataset is available in Nexus format as MorphoBank Project 6376, 'The centipede *Cryptops* from Baltic amber (Chilopoda: Scolopendromorpha): phylogenetic analysis using combined morphological and molecular data' (morphobank.org).

Molecular data and total-evidence phylogenetics

For the molecular data we focused on four loci used in previous scolopendromorph phylogenetic analyses (Vahtera *et al*., 2012, 2013): nuclear ribosomal RNA genes 18S rRNA and 28S rRNA, and two mitochondrial genes, the ribosomal RNA gene 16S rRNA and the protein-encoding gene cytochrome *c* oxidase subunit I (COI hereafter). Most species were represented by a single terminal, but *Scolopocryptops melanostomus* and *S. mexicanus* were represented by two terminals each, capturing some intraspecific variation. All sequences were downloaded from GenBank, mostly from previous work by the authors (Edgecombe *et al*., 2012, 2020; Vahtera *et al*., 2012), and individual loci/fragments were aligned with MAFFT version 7 (https://mafft.cbrc.jp/alignment/server/index.html) (Katoh & Standley, 2013; Kuraku *et al*., 2013; Katoh *et al*., 2019) (options—thread 4—threadtb 5—threadit 0—reorder—op 5.0—auto), as these parameters work well with a variety of data types.

For 28S rRNA, we relied on the D3 region defined between primers 28Sa and 28Sb (Whiting *et al*., 1997), which was available for most of the terminals selected, and therefore longer sequences were trimmed to this fragment prior to multiple sequence alignment. All three ribosomal RNA fragments were further subjected to trimming with Gblocks (Castresana, 2000; Talavera

TABLE 1. Extant taxa included in the combined morphological and molecular phylogenetic analysis, indicating the availability of morphological characters and molecular sequence data for each species.

Taxonomy	Species	Voucher	Country	18S	28S	16S	COI
Cryptopidae	*Cryptops* (*Cryptops*) *hortensis*	MCZ:IZ:130582	United Kingdom	**JX422708**	**JX422582**	**JX422684**	**JX422662**
	Cryptops (*Cryptops*) *lamprethus*	MCZ:IZ:130584	New Zealand	**JX422709**	**JX422583**	**JX422685**	**JX422663**
	Cryptops (*Cryptops*) *niuensis*	MCZ:IZ:130589	Fiji	**JX422710**	**JX422584**	**JX422686**	**JF273294**
	Cryptops (*Trigonocryptops*) *sarasini*	MCZ:IZ:130605	New Caledonia	**JX422711**	**JX422585**	**JX422687**	**JX422664**
	Cryptops (*Paracryptops*) *weberi*	MCZ:IZ:130609	Indonesia	**HQ402518**	**HQ402535**	**KF676464**	**HQ402551**
	Cryptops (*Cryptops*) *parisi*	MCZ:IZ:130592	United Kingdom	**KF676409**	**KF676356**	**KF676460**	**KF676502**
	Cryptops (*Cryptops*) *anomalans*	MCZ:IZ:131458	United Kingdom	**KF676406**	**KF676353**	**KF676457**	**KF676499**
	Cryptops (*Cryptops*) *punicus*	MCZ:IZ:130604	Italy	**KF676410**	**-**	**KF676461**	**KF676503**
	Cryptops (*Cryptops*) *doriae*	MCZ:IZ:130578	Thailand	**KF676407**	**KF676354**	**KF676458**	**KF676500**
	Cryptops (*Cryptops*) *trisulcatus*	MCZ:IZ:130606	Italy	**AF000775**	**AF000783**	**HQ402493**	**HQ402544**
	Cryptops (*Paracryptops*) *indicus*	MCZ:IZ:130608	Vietnam	**KF676412**	**KF676357**	**KF676463**	**KF676505**
	Cryptops (*Trigonocryptops*) *galatheae*	MCZ:IZ:130581	Argentina	**KF676408**	**KF676355**	**KF676459**	**KF676501**
	Cryptops (*Cryptops*) *australis*	AM KS 58458	Australia	**AY288692**	**AY288708**	**AY288723**	**-**
	Cryptops (*Cryptops*) *legagus*	IG130501C	Botswana	**MT925726**	**MT928357**	**MT925727**	**MT920964**
	Cryptops (*Cryptops*) *typhloporus*	MCZ:IZ:130607	South Africa	**KF676411**	**-**	**KF676462**	**KF676504**
	Cryptops (*Trigonocryptops*) *spinipes*	AM KS 58457	Australia	**AY288693**	**AY288709**	**AY288724**	**AY288743**
Plutoniumidae	*Plutonium zwierleini*	CLB00012	Italy	**LN890290**	**LN890291**	**LN890289**	**LN890292**
	Theatops erythrocephalus	MCZ:IZ:130611	Portugal	**AF000776**	**HM453279**	**JX422689**	**JX422665**
	Theatops posticus	MCZ:IZ:130612	USA	**JX422712**	**-**	**JX422688**	**JX422666**
Scolopocryptopidae, Newportiinae	*Newportia* (*Ectonocryptoides*) *quadrimeropus*	MCZ:IZ:130826	Mexico	**HQ402511**	**KF676358**	**HQ402494**	**HQ402546**
	Newportia divergens	MCZ:IZ:130772	Mexico	**JX422713**	**JX422586**	**JX422690**	**JX422667**
	Newportia ernsti ernsti	MCZ:IZ:130773	Dominican Republic	**JX422715**	**JX4225877**	**JX422692**	**JX422669**
	Newportia longitarsis stechowi	AMNH_LP3871	French Guiana	**JX422716**	**JX422588**	**JX422693**	**JX422670**
	Newportia monticola	MCZ:IZ:130778	Colombia	**JX422717**	**JX422589**	**JX422694**	**JX422671**
	Newportia stolli	MCZ:IZ:130787	Guatemala	**JX422719**	**JX422591**	**JX422696**	**JX422673**
	Newportia (*Tidops*) *collaris*	MCZ:IZ:126830	Brazil	**KF676415**	**KF676361**	**KF676467**	**KF676508**
Scolopocryptopidae, Scolopocryptopinae	*Scolopocryptops macrodon*	MCZ:IZ:130814	Guyana	**JX422721**	**-**	**JX422699**	**JX422675**
	Scolopocryptops melanostomus	AMNH LP6249	Costa Rica	**JX422722**	**-**	**JX422700**	**JX422676**
	Scolopocryptops melanostomus	MCZ:IZ:130815	Fiji	**JX422723**	**-**	**JX422701**	**JX422677**
	Scolopocryptops mexicanus	MCZ:IZ:130810	Colombia	**JX422724**	**JX422592**	**JX422702**	**JX422678**
	Scolopocryptops mexicanus	MCZ:IZ:130812	Ecuador	**JX422725**	**JX422593**	**JX422703**	**JX422679**
	Scolopocryptops miersii	MCZ:IZ:130729	Brazil	**JX422720**	**KF676364**	**JX422697**	**JX422674**
	Scolopocryptops nigridius	MCZ:IZ:130806	USA	**JX422726**	**JX422594**	**JX422704**	**JX422680**
	Scolopocryptops nipponicus	MCZ:IZ:130804	Japan	**JX422727**	**JX422595**	**JX422705**	**JX422681**
	Scolopocryptops sexspinosus	MCZ:IZ:131450	USA	**AY288694**	**AY288710**	**AY288726**	**AY288745**
	Scolopocryptops rubiginosus	MCZ:IZ:130823	Taiwan	**JX422728**	**-**	**JX422706**	**JX422682**
	Scolopocryptops spinicaudus	AMNH_IZC_00146514	USA	**JX422729**	**JX422596**	**JX422707**	**JX422683**
Scolopendridae, Otostigminae, Otostigmini	*Otostigmus* (*Otostigmus*) *astenus*	MCZ:IZ:130669	Fiji	**HQ402515**	**HQ402532**	**HM453221**	**HM453312**
Scolopendridae, Scolopendrinae, Scolopendrini	*Cormocephalus aurantiipes*	MCZ:IZ:130628	Australia	**HQ402509**	**KF676388**	**HQ402492**	**HQ402543**

TABLE 2. Evolutionary model selection using Bayesian Information Criterion (BIC) results. Full partition model BIC score: 52258.406 (LnL: -25667.945 df:114).

No. Model	Score	TreeLen	Charset +R5 reinitialized from +R4 with factor 0.500
1 TVM+F+I+G4	11698.934	5.302	part1
2 TN+I+G4	11965.254	0.384	part2
3 HKY+R2	2918.464	0.92	part3
4 GTR+F+I+G	22988.815	19.872	part4
5 MK+FQ+ASC+G4	1964.544	2.695	part5

& Castresana, 2007), allowing for gap positions for half of the sequences and a minimum length of a block of 3, with the rest of parameters following the defaults implemented in NGPhylogeny.fr (Lemoine *et al*., 2019) (https://ngphylogeny.fr/tools/tool/276/form). Because no internal gaps were inferred for the COI data set, no further trimming was done for this marker.

For 18S rRNA, 39 sequences (the 37 extant species with two represented by two individuals each) and 1,857 positions in the first alignment resulted in 1,814 positions (97%) in 15 selected blocks; for 28S rRNA, 31 sequences and 854 positions in the first alignment file resulted in 255 positions (29%) in four selected blocks; and for 16S rRNA, 38 sequences and 595 positions in the first alignment file resulted in 369 positions (62%) in 10 selected blocks. The COI alignment had a length of 769 positions. The combined alignment contained 3,208 positions. Individual gene fragments were concatenated with SequenceMatrix 1.8 (Vaidya *et al*., 2011). FASTA files of the aligned sequences are available on the Harvard Dataverse as https://doi.org/10.7910/DVN/NR3MJJ.

Phylogenetic analyses of the individual loci were conducted to test for systematically implausible relationships suggestive of potential sequencing mistakes such as contamination. Individual and concatenated loci, as well as the combined molecular and morphological data matrices were run in IQ-TREE 3 (Wong *et al*., 2025) with automated model selection (Kalyaanamoorthy *et al*., 2017). For the combined analyses we chose an edge-unlinked partition model, where each partition has its own set of branch lengths, and auto model selection with free rate heterogeneity (Table 2). Nodal support was assessed with 1,000 replicates of ultrafast bootstrapping (UFBS) (Hoang *et al*., 2018).

Systematic palaeontology

Order Scolopendromorpha Pocock, 1895–1896
Family Cryptopidae Kohlrausch, 1881
Genus *Cryptops* Leach, 1814
Subgenus *Cryptops* (*Cryptops*) Leach, 1814

***Cryptops* (*Cryptops*) sp.**
(Figs 1–4)

NHMUK 014872695

Length (anterior margin of cephalic plate to posterior margin of ultimate sternite) 15 mm (Fig. 1). Antennae complete, each composed of 17 elongate oval articles, all subequal in size apart from more elongate terminal article; setal density increases gradually distally with fine setae becoming progressively denser toward terminal articles (Fig. 2C). Cephalic plate ovoid; 1 mm long and 0.8 mm wide, anterior and lateral margins curved, dorsal posterior edge truncate (Fig. 2A). Cephalic plate and tergites mostly brown, with white granules surrounded by light blue attributed to decay. Eyes absent, with no relief or change in pigment or sclerotization in the expected position of lenses. Cephalic plate overlapping anterior margin of T1; T1 bearing a distinct obtuse V-shaped anterior transverse suture. Trunk with 21 leg-bearing segments. Paramedian sutures complete from T4 onward, nearly complete on T3, incomplete on T2; oblique sutures from T4; lateral crescentic sulci from at least T9. Strong pre- and metatergites visible from T2. T19–T21 poorly preserved, with tergites either absent or in degraded condition (Fig. 1). Locomotory legs composed of five segments and slender pretarsal claw; tarsi unjointed, without a suture or flexure; legs bearing many strong pigmented setae of similar length and diameter from prefemur to tarsus. Coxopleural pores visible on both ultimate legs, the left better preserved, displaying *ca.* 30 mostly uniformly sized pores (Fig. 2B); posterior pore-free area short, less than 15% length of coxopleuron. No spine-like setae observed within the pore field. Posterior margin of coxopleuron transverse, without a coxopleural process. Ultimate legs incompletely preserved (prefemur to partial tibia only); prefemur three times longer than wide; prefemur and femur with robust, spiniform setae on lateral side and their bases on ventral sides anchored in surrounding white decay residue (Figs 1, 2B). Cephalic plate and tergites sparsely scattered with long setae visible under light microscopy.

FIGURE 1. *Cryptops* sp., specimen NHMUK 014872695. Dorsal habitus. Scale bar: 1 mm.

Ventral side of specimen incomplete, owing to its orientation during resin entrapment and sectioning; details of ventral surface of sternites, labrum, maxillae and forcipular segment not preserved in plane of section.

GPI C. Gröhn 623

Length (anterior margin of cephalic plate to posterior margin of tergite 12) 6.4 mm (Fig. 3C). Antennae complete, with 17 oval articles; all articles subequal in size; setal density increases gradually distally with fine setae becoming progressively denser toward terminal articles. Cephalic plate ovoid, 0.8 mm long and 0.7 mm wide, anterior and lateral margins rounded, posterior margin truncate (Fig. 4A). Cephalic plate flat, bearing a shallow transverse groove near posterior margin, lacking longitudinal sutures both anteriorly and posteriorly; cephalic plate overlapping anterior margin of T1. Eyes absent, with no relief or change in pigment or sclerotization in the expected position of lenses. Robust forcipules, with a distinguishable hinge between femur and tibia (Fig. 3A, B). Forcipular coxosternite short, broad, lacking visible sutures; anterior margin smooth, bearing a shallow medial diastema (Fig. 4B); marginal or submarginal setae not observed. First maxillae poorly preserved; coxae discernible, exhibiting a weak medial incision and a pronounced positive relief visible on ventral surface. Second maxillae with three articles and claw (Fig. 4C), the latter distally hooked. Labrum indistinct, not separable from surrounding cephalic structures under current scan resolution. T1 with a well-defined obtuse V-shaped anterior transverse suture (Figs 3A, 4A), lacking paramedian or other sutures. Trunk of at least 13 leg-bearing segments. Strong pre- and metatergites visible from T2. Tergites with complete paramedian sutures from T4 onwards; oblique sutures from T4; paramedian sulci from T3. Lateral crescentic sulci hardly identifiable. Sutures poorly distinguishable under light microscopy and not resolved in 3D tomography. Single spheroidal spiracle discerned in pleuron on right side of eighth leg-bearing segment. Details of sternites not preserved. Locomotory legs composed of five segments and slender pretarsal claw; tarsi unjointed, without a suture or flexure; claw lacking accessory spurs. On right side, procoxa and metacoxa preserved, both elongated and ovoid; eucoxae (superior and inferior) likewise elongate, articulating near the trochanter (Fig. 4D). Cephalic plate, forcipules and tergites sparsely scattered with long setae visible under light microscopy.

Remarks

Both specimens have the cuticle partially preserved; the internal body structure is largely hollow, indicating decomposition. White, amorphous material surrounding both fossils is interpreted as a byproduct of decay; some setae are embedded within this material.

The two specimens are attributed to the genus *Cryptops* based on the following characters: lack of eyes; basal antennal articles bearing numerous long setae dorsally, with a gradation towards shorter, denser setae distally along the antenna; strong pre- and metatergites, and presence of oblique sutures and lateral crescentic sulci on the tergites. NHMUK 014872695 provides the additional

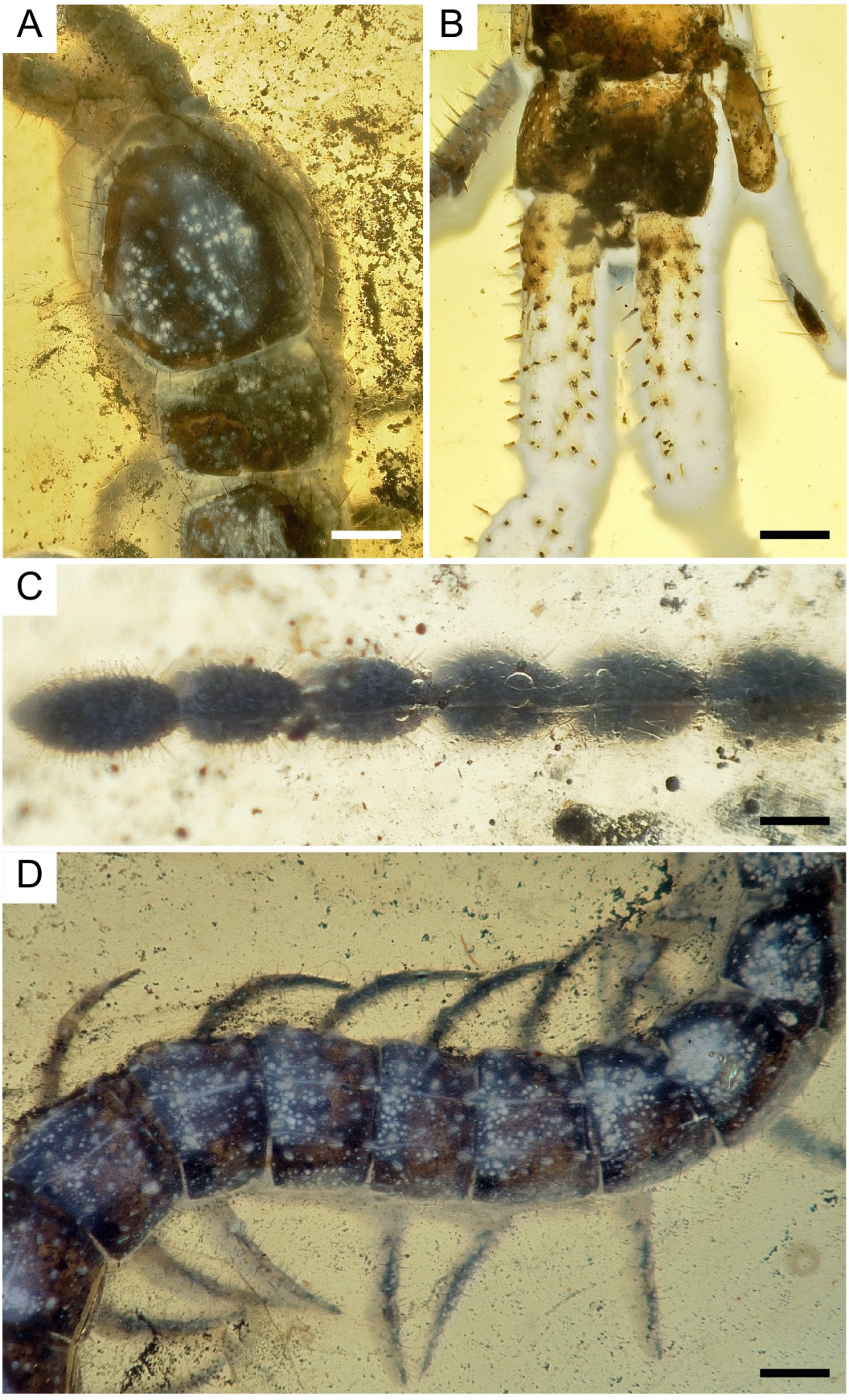

FIGURE 2. *Cryptops* sp., specimen NHMUK 014872695. **A**, Dorsal view of the head and T1. **B**, Dorsal view of the interior of the ventral part of segment 21 and ultimate leg-bearing segment (tergites and dorsal surface of leg removed). **C**, Dorsal view of articles 12 to 17 of the right antenna. **D**, Dorsal view of trunk segments 8 to 14. Scale bars: 0.25 mm (**A**, **B**); 0.1 mm (**C**); 0.4 mm (**D**).

FIGURE 3. *Cryptops* sp., specimen GPI C. Gröhn 623. **A**, **B**, Oblique dorsal and ventral views, respectively of the head and forcipular segment. **C**, Partly dorsal habitus. Scale bars: 0.25 mm **(A)**; 0.2 mm (**B**); 0.8 mm (**C**).

diagnostic characters of 21 leg-bearing segments, lack of a coxopleural process, and robust, spiniform setae on the prefemur and femur of the ultimate legs, whereas GPI C. Gröhn 623 demonstrates the characteristic short forcipular coxosternite, with a smooth, weakly bilobate anterior margin lacking tooth-plates, and absence of a forcipular trochanteroprefemoral process.

The two amber-hosted specimens are grouped as the same species based on sharing certain characters that are useful in delimiting extant species of *Cryptops*, notably the lack of longitudinal sutures on the cephalic plate and sutures on T1 being limited to a strongly defined V-shaped anterior transverse suture; W- or X-shaped and/or paramedian sutures behind the transverse suture are wholly lacking. Among extant species, the combination of a lack of longitudinal sutures on the cephalic plate, the cephalic plate overlapping the anterior margin of T1, and sutures on T1 being limited to an anterior transverse suture with an obtuse V shape may be matched only by *Cryptops neocaledonicus muchmorei* Lewis, 1989, from the U.S.

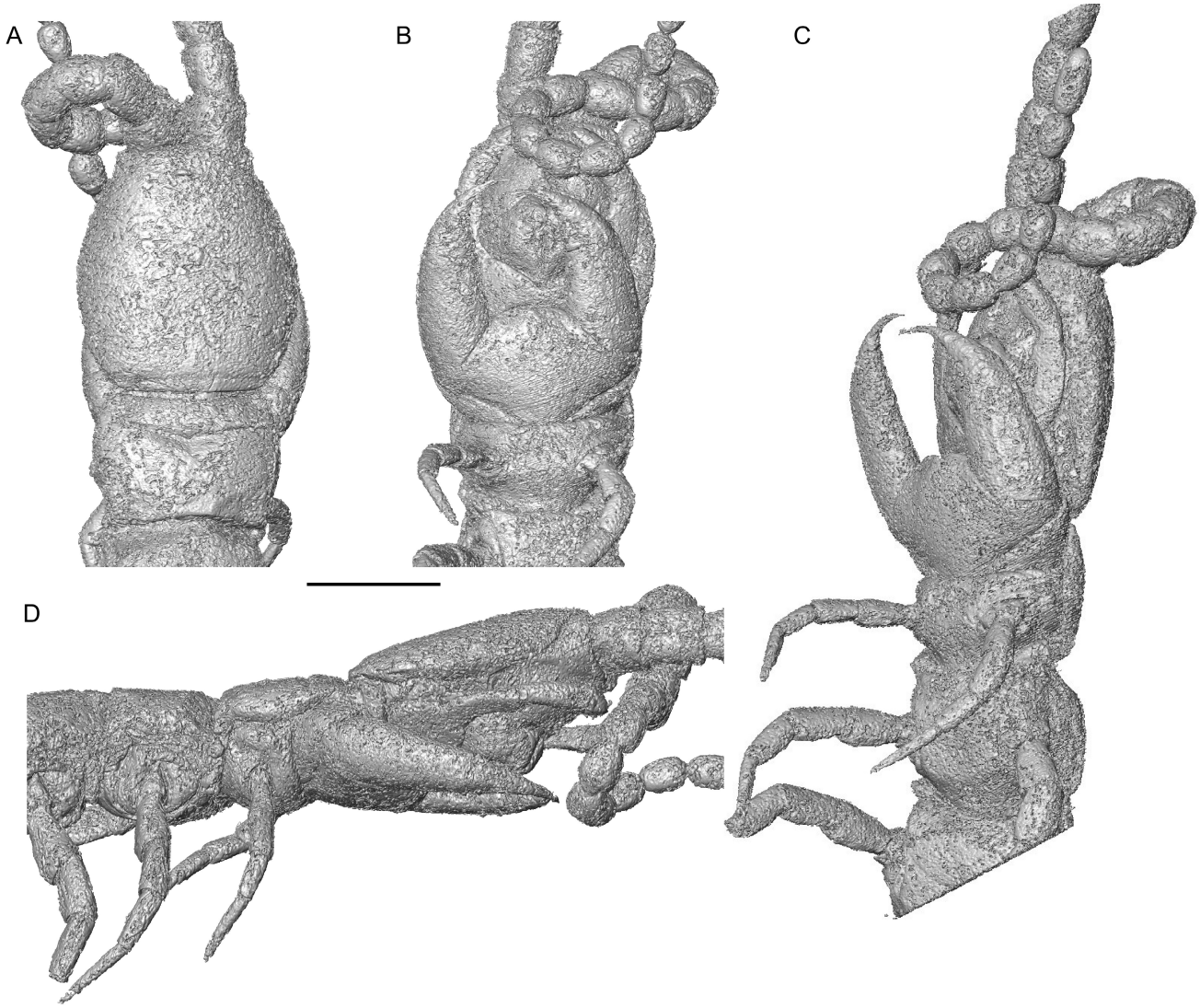

FIGURE 4. *Cryptops* sp., specimen GPI C. Gröhn 623. Microtomographic reconstructions. **A**, **B**, Dorsal and ventral views, respectively, of head and anterior part of trunk. **C**, Ventrolateral view of the head and anterior part of trunk. **D**, Lateral view of head and trunk segments 1–3. Scale bars: 0.5 mm.

Virgin Islands (Lewis, 1989). Specific distinctness of the Baltic amber material from that subspecies can, however, be defended by the slenderer prefemur and femur of the ultimate leg. Without information on some standard species-level taxonomic characters, notably the saw teeth on the ultimate leg, we have chosen not to formally name the fossil species. The closest taxonomic comparisons are with species of the nominate (and by far most speciose) subgenus, *C*. (*Cryptops*). The lack of longitudinal sutures on the cephalic plate and undivided tarsi of the locomotory legs are more consistent with that subgenus than with *C*. (*Trigonocryptops*), the size of the forcipular tarsungulum and lack of rounded hyaline projections on the forcipular coxosternite rule out membership in *C*. (*Paracryptops*), and the hooked distal tip of a "normal"-sized second maxillary claw distinguishes the Eocene species from the monotypic *C*. (*Haplocryptops*).

Combined morphological and molecular phylogenetics

The maximum likelihood tree (Fig. 5) recovers the major clades (families and subfamilies) of Tykhepoda with strong support (UFBoot 100% for Plutoniumidae, 99% for Scolopocryptopidae, 98% for Scolopocryptopinae, 100% for Newportiinae, 100% for Cryptopidae). Within *Scolopocryptops*, the two clades recovered in previous morphological and molecular phylogenies, one grouping North American/Asian species and the other uniting Neotropical/West African species (Edgecombe *et al*., 2012), are both strongly supported (UFBoot 99% and 98%, respectively).

The Baltic amber *Cryptops* species is robustly recovered within total-group *Cryptops* (UFBoot 100%), with weak support for it nesting a node crownward of the deepest split within *Cryptops*. Relationships between extant species of *Cryptops* are mostly identical to those

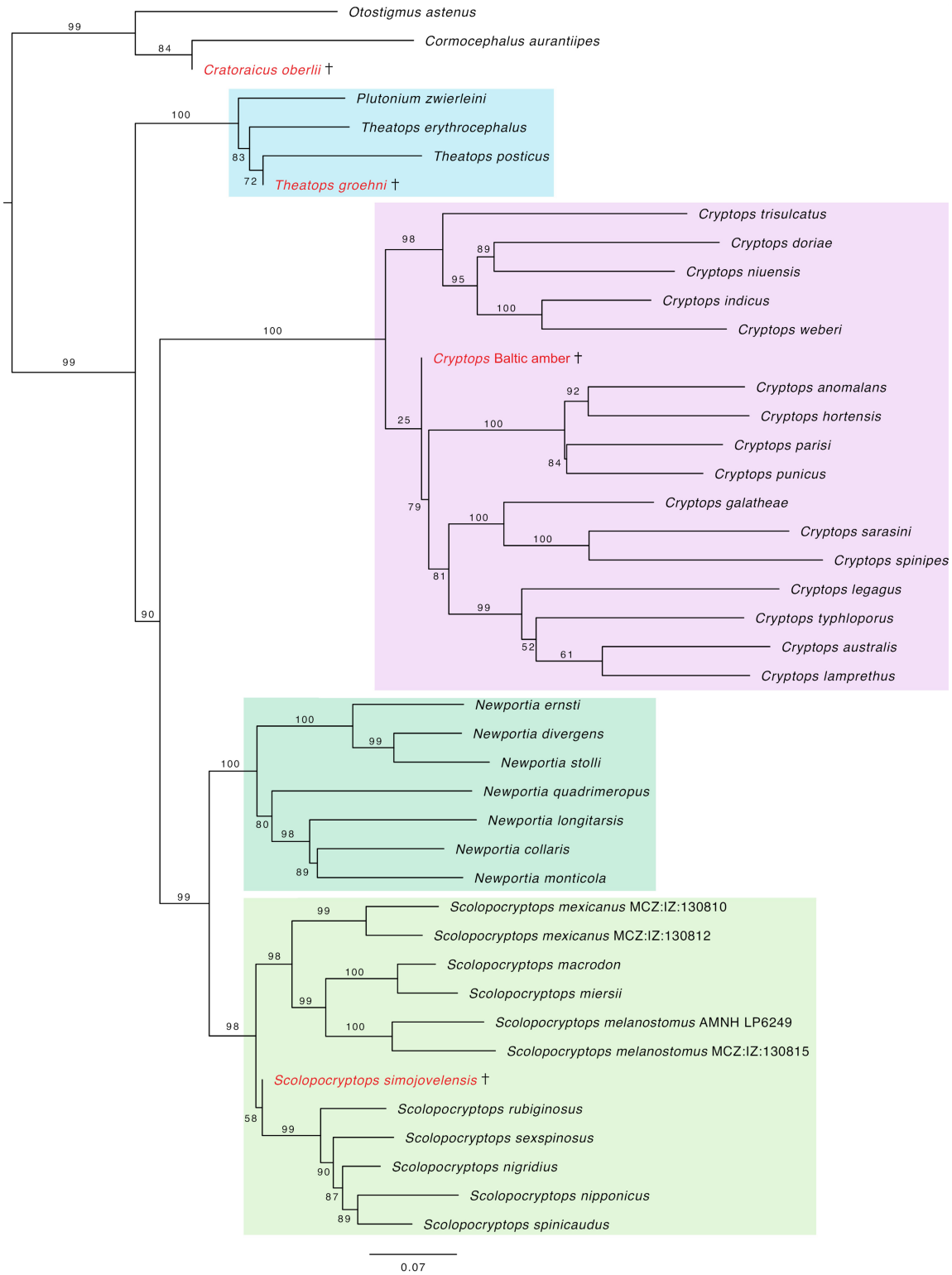

FIGURE 5. Maximum likelihood tree for combined morphological and molecular data. Extinct species indicated by daggers. Numbers on nodes are ultrafast bootstrap support.

depicted by Edgecombe *et al*. (2020) in a molecules-only analysis. As found therein, the two sampled species of *C*. (*Paracryptops*), *i.e*., *C. indicus* and *C. weberi*, and three sampled species of *C*. (*Trigonocryptops*) (*C. galatheae*, *C. sarasini*, *C. spinipes*) unite as clades with UFBoot 100% in both cases. The nominate subgenus *C*. (*Cryptops*) is paraphyletic with respect to both of those monophyletic subgenera.

Clades within *C*. (*Cryptops*) show considerable geographic structure. A Palaearctic clade (UFBoot 100%) groups *C. anomalans*, *C. hortensis*, *C. parisi* and *C. punicus*. An Asian/western Pacific clade unites *C. doriae*

and *C. niuensis*, two species whose close affinity was anticipated by morphology (Lewis, 2013). An Australasian clade of *C. australis* and *C. lamprethus* unites with species from southern Africa (*C. typhloporus* and *C. legagus*) with UFBoot 99%. Should the latter reflect Gondwanan vicariance, we expect that the deep nodes within *Cryptops* considerably predate the minimum divergence date provided by the Eocene fossil (see discussion below).

Discussion

The scarcity of records of *Cryptops* in amber may be in part related to habitat mismatch; in temperate areas, extant species of the genus are usually collected under stones, under dead wood, in leaf litter, and in dead wood or under its bark (Barber, 2002), rather than on or under the bark of living trees. However, in tropical rainforest, *Cryptops* is common in epiphytes at low canopy height (Phillips *et al*., 2020), but these sites likely shelter them from resin.

As discussed above, the Eocene fossils are not formally named as a new species nor attributed to an extant species of *Cryptops*. The fossils code for a unique combination of morphological characters and the total-evidence maximum likelihood tree places the extinct species in an isolated systematic position rather than nesting with any single extant species. Among the species for which molecular data are available, the Baltic amber fossils share some characters with *C. trisulcatus,* which also has an obtuse V-shaped anterior transverse suture on the first tergite (Ribaut, 1915: fig. IX) and, like the fossils, a relatively elongate cephalic shield (Zalesskaya & Schileyko, 1991: fig. 13.1). However, the combined data do not identify these similarities as synapomorphies.

Previous molecular dating using the limited taxonomic sampling afforded by transcriptomic data dated the split between *C. anomalans* and *C. hortensis*, close relatives in the Palaearctic clade, to a midpoint in the Eocene, with a 95% highest posterior density spanning the latest Cretaceous to late Oligocene (Benavides *et al*., 2023). Murienne *et al*. (2010) dated the divergence between *C. australis* and *C. spinipes* to a midpoint in the Early Cretaceous (138 Ma) and the split of those Gondwanan species from the Palaearctic *C. trisulcatus* to the Jurassic (midpoint 164 Ma). Geographic patterns such as Gondwanan subclades noted above are consistent with these Mesozoic deep splits.

Conclusion

The two Eocene Baltic amber specimens described are confidently assigned to the genus *Cryptops* within the scolopendromorph family Cryptopidae. Diagnostic apomorphic characters and total-evidence phylogenetic analysis support this assignment. The quality of preservation hinders the ability to link these fossils to any recognized extant species, but observed characters show diagnostic differences compared to the morphology of known extant species. The placement of the amber-hosted fossils according to phylogenetic analysis provides a minimum divergence date for total-group *Cryptops* in the late Eocene (Priabonian) based on the age of Baltic amber.

Acknowledgments

C. V.-M.'s research in London was funded by an internship from Université Claude Bernard Lyon 1. We are grateful to Carsten Gröhn for loan of one of the two fossil specimens and to Richard Howard (The Natural History Museum) for curatorial support. This work was generously supported by the Imaging and Analysis Centre at the Natural History Museum; we thank Brett Clark, Agnese Lanzetti, and Madeleine Widdowson for assistance with microtomography, and Dana Perry for assistance with light microscopy. Referee George Popovici and Handling Editor Chenyang Cai provided helpful feedback on the manuscript.

References

Bachofen-Echt, A. (1942) Über Myriapoden des Bernsteins. *Palaeobiologica*, 7 (3), 394–403.

Barber, A.D. (2002) *Atlas of the centipedes of Britain and Ireland*. Field Studies Council, Telford, 390 pp.

Benavides, L.R., Edgecombe, G.D. & Giribet, G. (2023) Re-evaluating and dating myriapod diversification with phylotranscriptomics under a regime of dense taxon sampling. *Molecular Phylogenetics and Evolution*, 178, 107621. https://doi.org/10.1016/j.ympev.2022.107621

Cadenas-Amaya, S., Riquelme, F., Hernández-Patricio, M. & Cupul-Magaña, F. (2025) A checklist of centipedes in Mexican amber. *Paleontología Mexicana*, 14 (2), 107–120. https://doi.org/10.22201/igl.05437652e.2025.14.2.405

Castresana, J. (2000) Selection of conserved blocks from multiple alignments for their use in phylogenetic analysis. *Molecular Biology and Evolution*, 17, 540–552. https://doi.org/10.1093/oxfordjournals.molbev.a026334

Edgecombe, G.D., Akkari, N., Netherlands, E.C. & Du Preez, G. (2020) A troglobitic species of the centipede *Cryptops* (Chilopoda, Scolopendromorpha) from northwestern Botswana. *ZooKeys*, 977, 25–40. https://doi.org/10.3897/zookeys.977.57088

Edgecombe, G.D., Strange, S.E., Popovici, G., West, T. & Vahtera, V. (2023) An Eocene fossil plutoniumid centipede: A new species of *Theatops* from Baltic amber (Chilopoda: Scolopendromorpha). *Journal of Systematic Palaeontology*, 21 (1), 2228796, 1–17.
https://doi.org/10.1080/14772019.2023.2228796

Edgecombe, G.D., Vahtera, V., Stock, S.R., Kallonen, A., Xiao, X., Rack, A. & Giribet, G. (2012) A scolopocryptopid centipede (Chilopoda: Scolopendromorpha) from Mexican amber: synchrotron microtomography and phylogenetic placement using a combined morphological and molecular dataset. *Zoological Journal of the Linnean Society*, 166, 768–786.
https://doi.org/10.1111/j.1096-3642.2012.00860.x

Haug, J.T., Haug, C., Schweigert, G. & Sombke, A. (2014) The evolution of centipede venom claws—Open questions and possible answers. *Arthropod Structure & Development*, 43 (1), 5–16.
https://doi.org/10.1016/j.asd.2013.10.006

Hoang, D.T., Chernomor, O., von Haeseler, A., Minh, B.Q. & Vinh, L.S. (2018) UFBoot2: Improving the ultrafast bootstrap approximation. *Molecular Biology and Evolution*, 35, 518–522.
https://doi.org/10.1093/molbev/msx281

Kalyaanamoorthy, S., Minh, B.Q., Wong, T.K.F., von Haeseler, A. & Jermiin, L.S. (2017) ModelFinder: fast model selection for accurate phylogenetic estimates. *Nature Methods*, 14, 587–589.
https://doi.org/10.1038/nmeth.4285

Katoh, K., Rozewicki, J. & Yamada, K.D. (2019) MAFFT online service: multiple sequence alignment, interactive sequence choice and visualization. *Briefings in Bioinformatics*, 20, 1160–1166.
https://doi.org/10.1093/bib/bbx108

Katoh, K. & Standley, D.M. (2013) MAFFT multiple sequence alignment software version 7: Improvements in performance and usability. *Molecular Biology and Evolution*, 30, 772–780.
https://doi.org/10.1093/Molbev/Mst010

Kuraku, S., Zmasek, C.M., Nishimura, O. & Katoh, K. (2013) aLeaves facilitates on-demand exploration of metazoan gene family trees on MAFFT sequence alignment server with enhanced interactivity. *Nucleic Acids Research*, 41, W22–W28.
https://doi.org/10.1093/nar/gkt389

Lemoine, F., Correia, D., Lefort, V., Doppelt-Azeroual, O., Mareuil, F., Cohen-Boulakia, S. & Gascuel, O. (2019) NGPhylogeny.fr: new generation phylogenetic services for non-specialists. *Nucleic Acids Research*, 47, W260–W265.
https://doi.org/10.1093/nar/gkz303

Lewis, J.G.E. (1989) The scolopendromorph centipedes of St John, U.S. Virgin Islands collected by Dr W. B. Muchmore. *Journal of Natural History*, 23, 1003–1016.
https://doi.org/10.1080/00222938900770921

Lewis, J.G.E. (2009) A review of some characters used in the taxonomy of *Cryptops* (subgenus *Cryptops*) (Chilopoda: Scolopendromorpha: Cryptopidae). *Soil Organisms*, 81 (3), 505–518.

Lewis, J.G.E. (2013) A review of the species in the genus *Cryptops* Leach, 1815 from the Old World and the Australasian region related to *Cryptops* (*Cryptops*) *doriae* Pocock, 1891 (Chilopoda: Scolopendromorpha: Cryptopidae). *Zootaxa*, 3683 (1), 1–34.
https://doi.org/10.11646/zootaxa.3683.1.1

Maddison, W.P. & Maddison, D.R. (2025) Mesquite: a modular system for evolutionary analysis. Version 3.81. (Available from: http://www.mesquiteproject.org).

Mundel, P. (1979) The centipedes (Chilopoda) of the Mazon Creek. *In*: Nitecki, M.H. (Ed.), *Mazon Creek fossils*. Academic Press, New York, pp. 361–378.
https://doi.org/10.1016/B978-0-12-519650-5.50021-7

Murienne, J., Edgecombe, G.D. & Giribet, G. (2010) Including secondary structure, fossils and molecular dating in the centipede tree of life. *Molecular Phylogenetics and Evolution*, 57, 301–313.
https://doi.org/10.1016/j.ympev.2010.06.022

Phillips, J.W., Chung, A.Y.C., Edgecombe, G.D. & Ellwood, M.D.F. (2020) Bird's nest ferns promote resource sharing by centipedes. *Biotropica*, 52, 335–344.
https://doi.org/10.1111/btp.12713

Pocock, R.I. (1891) XXIV.—Notes on the synonymy of some species of Scolopendridæ, with descriptions of new genera and species of the group. *Annals and Magazine of Natural History*, 7 (38), 221–231.
https://doi.org/10.1080/00222939109460598

Poinar, G.O. (1992) *Life in amber*. Stanford University Press, Palo Alto, 350 pp.
https://doi.org/10.1515/9781503623545

Ribaut, H. (1915) Biospeologica, XXXVI. Notostigmophora, Scolopendromorpha, Geophilomorpha (Myriapodes) (Première Série). *Archives de Zoologie Expérimentale et Générale*, 55, 323–346.

Ross, A.J., Bojarski, B. & Szwedo, J. (2026) A critical review of the age of Baltic amber from the Samland Peninsula, Russia. *Earth and Environmental Science Transactions of the Royal Society of Edinburgh, First View*, 1–14.
https://doi.org/10.1017/S1755691025100960

Schileyko, A., Vahtera, V. & Edgecombe, G.D. (2020) An overview of the extant genera and subgenera of the order Scolopendromorpha (Chilopoda): a new identification key and updated diagnoses. *Zootaxa*, 4825 (1), 1–64.
https://doi.org/10.11646/zootaxa.4825.1.1

Talavera, G. & Castresana, J. (2007) Improvement of phylogenies after removing divergent and ambiguously aligned blocks from protein sequence alignments. *Systematic Biology*, 56, 564–577.
https://doi.org/10.1080/10635150701472164

Vahtera, V., Edgecombe, G.D. & Giribet, G. (2012) Evolution of blindness in scolopendromorph centipedes (Chilopoda: Scolopendromorpha): Insight from an expanded sampling of molecular data. *Cladistics*, 28, 4–20. https://doi.org/10.1111/j.1096-0031.2011.00361.x

Vahtera, V., Edgecombe, G.D. & Giribet, G. (2013) Phylogenetics of scolopendromorph centipedes: can denser taxon sampling improve an artificial classification? *Invertebrate Systematics*, 27, 578–602. https://doi.org/10.1071/IS13035

Vaidya, G., Lohman, D.J. & Meier, R. (2011) SequenceMatrix: concatenation software for the fast assembly of multi-gene datasets with character set and codon information. *Cladistics*, 27, 171–180. https://doi.org/10.1111/j.1096-0031.2010.00329.x

Whiting, M.F., Carpenter, J.M., Wheeler, Q.D. & Wheeler, W.C. (1997) The Strepsiptera problem: phylogeny of the holometabolous insect orders inferred from 18S and 28S ribosomal DNA sequences and morphology. *Systematic Biology*, 46, 1–68. https://doi.org/10.1093/sysbio/46.1.1

Wolfe, A.P., Tappert, R., Muehlenbachs, K., Boudreau, M., McKellar, R.C., Basinger, J.F. & Garrett, A. (2009) A new proposal concerning the botanical origin of Baltic amber. *Proceedings of the Royal Society B: Biological Sciences*, 276 (1672), 3403–3412. https://doi.org/10.1098/rspb.2009.0806

Wong, T.K.F., Ly-Trong, N., Ren, H., Baños, H., Roger, A.J., Susko, E., Bielow, C., Maio, N.D., Goldman, N., Hahn, M.W., Huttley, G., Lanfear, R. & Minh, B.Q. (2025) IQ-TREE 3: Phylogenomic inference software using complex evolutionary models. *EcoEvoRxiv*. https://doi.org/10.32942/X2P62N

Zalesskaya, N.T. & Schileyko, A.A. (1991) [*The scolopendromorph centipedes (Chilopoda, Scolopendromorpha)*.] Nauka Publishing, Moscow, 110 pp. [In Russian]

Appendix 1: Newly added taxa

15 taxa were added to the original 29-taxon matrix of Edgecombe *et al*. (2023). Added taxa in bold. Fossil taxa indicated by dagger (†).

1. *Otostigmus astenus*
2. *Cormocephalus aurantiipes*
3. *Cratoraricrus oberlii*†
4. *Theatops erythrocephalus*
5. *Theatops groehni*†
6. *Theatops posticus*
7. *Plutonium zwierleini*
8. ***Cryptops anomalans***
9. ***Cryptops australis***
10. ***Cryptops doriae***
11. ***Cryptops galatheae***
12. *Cryptops hortensis*
13. *Cryptops lamprethus*
14. ***Cryptops legagus***
15. ***Cryptops niuensis***
16. ***Cryptops parisi***
17. ***Cryptops punicus***
18. *Cryptops sarasini*
19. ***Cryptops spinipes***
20. ***Cryptops trisulcatus***
21. ***Cryptops typhloporus***
22. ***Cryptops indicus***
23. *Cryptops weberi*
24. ***Cryptops* sp. Baltic Amber**†
25. *Newportia* (*Newportia*) *divergens*
26. *Newportia* (*Newportia*) *ernsti ernsti*
27. *Newportia* (*Newportia*) *longitarsis stechowi*
28. *Newportia* (*Newportia*) *monticola*
29. *Newportia* (*Ectonocryptoides*) *quadrimeropus*
30. *Newportia* (*Newportia*) *stolli*
31. ***Newportia* (*Tidops*) *collaris***
32. *Scolopocryptops macrodon*
33. *Scolopocryptops melanostomus*
34. *Scolopocryptops miersii*
35. *Scolopocryptops mexicanus*
36. *Scolopocryptops nigridius*
37. ***Scolopocryptops nipponicus***
38. *Scolopocryptops rubiginosus*
39. *Scolopocryptops sexspinosus*
40. *Scolopocryptops simojovelensis*†
41. *Scolopocryptops spinicaudus*

Appendix 2: Morphological characters

The morphological dataset analysed in this study adds eight characters to the 53-character matrix of Edgecombe *et al*. (2023). Data in nexus format available as MorphoBank Project 6376.

1. Number of pedigerous post-forcipular segments—(0) 21; (1) 23

2. Segmental distribution of spiracles—(0) restricted to trunk segments with long tergites excluding segment 7; (1) restricted to trunk segments with long tergites including segment 7; (2) present on all trunk segments except first and last

3. Eyes—(0) absent; (1) cluster of four ocelli

4. Desclerotised ocular patches—(0) absent; (1) present

5. Number of sparsely hirsute basal antennal articles—(0) at least three sparsely hirsute articles; (1) basal articles with numerous setae dorsally, with gradational trend to distal articles with shorter, denser seta; (2) basal article alone sparsely hirsute dorsally; (3) basal two articles sparsely hirsute dorsally, third at least distally as densely hirsute as subsequent articles

6. Structure of antennal sensilla—(0) mostly normal trichoid sensilla; (1) mostly sensilla that project from a basal tubercle or collar

7. Longitudinal sutures on cephalic plate—(0) absent; (1) paired, confined to extremities of head plate; (2) paired, complete along entire length of head plate

8. Cephalic plate margination—(0) absent; (1) present

9. Extent of cephalic plate margination—(0) laterally only or incomplete posteriorly; (1) complete and continuous laterally and posteriorly. Inapplicable if character 8 is scored 0

10. Anterior setose area on clypeus delimited by sutures—(0) absent; (1) present

11. Notch in labral sidepiece—(0) absent; (1) present

12. Structure of claw of second maxillary telopodite—(0) robust median claw with a slender spine on each side; (1) pectinate claw; (2) hook-like claw with ventral flange; (3) two curved processes, one above the other

13. Tooth plates of forcipules—(0) plates with strongly chitinized tooth margins; (1) chitinized anterior margin of coxosternite without plates; (2) hyaline, lobate plates lacking teeth

14. Trochanteroprefemoral process on forcipule—(0) absent; (1) present

15. Size of forcipular tarsungulum—(0) long enough that left and right sides cross; (1) short tarsungula of left and right sides do not cross

16. Hinge between articles of forcipule—(0) hinge between femur and tibia; (1) hinge between trochanteroprefemur and tarsungulum; (2) hinge between trochanteroprefemur and tibia

17. Form of venom duct—(0) straight or arcuate; (1) serpentine

18. Shape of venom calyx—(0) ovoid; (1) elongated

19. Relationship between cephalic plate and T1—(0) cephalic plate overlapping anterior margin of T1; (1) T1 overlapping cephalic plate; (2) abutting each other without consistent overlap

20. Anterior transverse suture on T1—(0) absent; (1) present

21. Shape of anterior transverse suture on T1—(0) curved; (1) V-shaped. Inapplicable if character 20 is scored 0

22. Shape of median/paramedian sutures on T1—(0) absent; (1) X-shaped; (2) W-shaped; (3) inverted Y-shaped sutures; (4) paramedian sutures only

23. Pre- and metatergites—(0) pretergite and metatergite merged; (1) strong pretergite set off from metatergite by continuous, transverse suture

24. Completeness of paramedian sutures on tergum—(0) complete on at least some tergites; (1) none extending more than posterior one-third of tergite length

25. Crescentic sulci on tergites—(0) absent on all tergites; (1) present on most tergites

26. Tergite margination—(0) margins present on more than last tergite; (1) restricted to last tergite only

27. Shape of ultimate tergite—(0) not substantially longer than penultimate tergite; (1) nearly twice as long as penultimate tergite

28. Median suture on ultimate tergite—(0) absent; (1) present

29. Paramedian sutures on sternites—(0) absent; (1) present and complete

30. Line of skeletal thickening across sternites originating at coxa—(0) absent; (1) present

31. Endosternite—(0) absent; (1) present

32. Trigonal sutures delimiting endosternite in anterior part of trunk—(0) absent; (1) present. Inapplicable if character 31 is scored 0.

33. Setae on locomotory legs—(0) strong, numerous; (1) slender, sparse

34. Structure of tarsi of locomotory legs—(0) divided into two articles; (1) fused, at least internally

35. Tarsal spurs of locomotory legs—(0) absent; (1) present

36. Dorsolateral tibial spur—(0) absent on all locomotory legs; (1) present on one or more locomotory legs

37. Ventral tibial spur—(0) absent on all locomotory legs; (1) present on most locomotory legs

38. Strongly thickened, forcipulate ultimate leg—(0) absent; (1) present

39. Coxopleural process of ultimate leg—(0) absent; (1) present (represented at least by spur)

40. Abundance of coxopleural pores in large specimens—(0) few in number (40 or fewer); (1) numerous (50 or more)

41. Abundance of setae on coxopleural pore field in large specimens—(0) absent; (1) few setae (5 or fewer); (2) abundant setae (10 or more)

42. Length of posterior pore-free area on coxopleuron—(0) short (<15% length of coxopleuron); (1) long (>20% length of coxopleuron)

43. Embayment in posterodorsal margin of coxopleural pore field—(0) absent; (1) present

44. Armature of ventral side of ultimate leg prefemur—(0) spines and spinous processes absent, as on locomotory legs; (1) small spine or conical swelling at distal end of longitudinal ridge on prefemur and (variably) femur; (2) large spinous process(es); (3) spines in ordered dorsomedial, medial, ventromedial and ventrolateral rows; (4) many irregular spines

45. Arrangement of spinous processes on ultimate leg prefemur—(0) a few processes in an irregular row; (1) single large ventral process and smaller dorsomedial process. Inapplicable unless character 44 is scored 2.

46. Ventral spinose processes on ultimate leg femur—(0) absent; (1) present

47. Paired dorsodistal spinose processes on ultimate leg tibia—(0) absent; (1) present

48. Saw teeth on ventral side of ultimate leg tibia and tarsus I—(0) absent; (1) present

49. Saw tooth/teeth on ultimate leg femur—(0) absent; (1) one or two distally

50. Tarsomeres in tarsus 2 of ultimate leg—(0) undivided tarsus 2; (1) tarsus 2 with numerous tarsomeres

51. Definition of tarsomeres in tarsus 2 of ultimate leg—(0) regular tarsomere boundaries; (1) irregular tarsomere boundaries. Inapplicable if character 50 is scored 0.

52. Medial sclerotisation of labral part of epipharynx—(0) sclerotisation continuous from median tooth to border with clypeal part; (1) sclerotisation confined to region immediately proximal to median tooth, discontinuous with border with clypeal part

53. Node- or spine-like scales across proximal labral part of epipharynx—(0) absent; (1) present

54. Sensillar field(s) on clypeal part of epipharynx—(0) band of sensilla coeloconica medially, immediately proximal to spine field; (1) lenticular field of sensilla coeloconica immediately proximal to spine field; (2) crescentic field of sensilla coeloconica laterally; (3) large field of sensilla coeloconica across median clypeal part, separated from spine field by a substantial expanse that bears scattered pores

55. Paired lateral cluster of sensilla on clypeal part of epipharynx—(0) both groups positioned laterally, widely separated from each other; (1) positioned medially, with each group closely approximating each other near midline

56. Extent of lateral longitudinal bands of scales on clypeal part of epipharynx—(0) not confluent across midline; (1) confluent across midline, developed proximomedially as polygonal scales

57. Gizzard structure—(0) plicae covered with scales that each bear a single spine; (1) posterior part of foregut organised as a sieve with stiff, anteriorly-directed projections

58. Anterior gizzard projections with pigmented bases bearing spinose scales or spines, distal part translucent, tapering, bearing dense hairs—(0) absent; (1) present. Inapplicable if character 57 is scored 0.

59. Terminal part of large pineapple-shaped projections of gizzard—(0) projections evenly tapering, tip filamentous; (1) projection bifid, with a short conical tip emerging from the notch. Inapplicable if character 57 is scored 0.

60. Shape of main zone of sieve projections—(0) evenly curved; (1) kinked near midlength, with distal part more strongly directed forwards. Inapplicable if character 57 is scored 0.

61. Longitudinally patterned bands of trichomes on basal half of sieve projections—(0) absent (trichomes, if present, not patterned); (1) present. Inapplicable if character 57 is scored 0.